

Loss Analysis of Electric Motors in Hybrid Excavator

Akira TSUTSUI*¹, Ryo FUJISAWA*², Kazuhide SEKIYAMA*², Yoichiro YAMAZAKI*³, Seiji SAEKI*³, Dr. Kazushige KOIWAI*⁴

*¹ Applied Physics Research Laboratory, Technical Development Group

*² Mechanical Engineering Research Laboratory, Technical Development Group

*³ Advanced Technology Department, Design & Development Engineering Division, Global Engineering Center (GEC), KOBELCO CONSTRUCTION MACHINERY CO., LTD.

*⁴ Corporate Planning & Administration Department, KOBELCO CONSTRUCTION MACHINERY CO., LTD.

Kobelco Construction Machinery Co., Ltd. has launched a new 20 tonne hybrid excavator, equipped with two types of newly developed electric motors, namely, a permanent magnet type, flat, high-torque generator motor, and a compact high-output slewing motor. In an electric motor, iron loss and copper loss occur, and these losses increase as the internal temperature rises. Therefore, the challenge in making compact electric motors with high torque and high output is to release the heat generated inside the motors to the outside and to prevent their internal temperature from rising. A technique has been established for the coupled analysis of an electrical/magnetic circuit model and a heat transfer circuit model in an electric motor that enables an optimal design of the heat transfer path inside the motor, as well as making it possible to efficiently find an appropriate electromagnetic circuit for it. This has resulted in the development of electric motors with high torque density.

Introduction

Kobelco Construction Machinery Co., Ltd. has commercialized hybrid excavators, each with a diesel engine equipped with a generator motor for power assist, in which the slewing system, which used to be driven hydraulically, is driven electrically. The company has launched 8 tonne machines and 20 tonne machines into the market so far. These products, however, employ general purpose devices for their power electronics such as generators, slewing electric motors, and inverters; these devices are large and expensive. Also, exclusive designs that are different from those of the standard hydraulic excavators are increasingly being used for the main body of these excavators to accommodate the spaces for installing the power electronics devices, posing a challenge in terms of cost.

Hence, in the new 20 tonne hybrid excavator, each power electronics device was downsized with our own exclusive design. For example, the generator motor has been flattened, with higher torque, and built-in between the engine and hydraulic pump. In addition, the slewing electric motor was downsized with a higher output so that it can fit in the installation space in each slewing hydraulic motor.

In this development, an analysis technology

was established to quickly verify the output performance, efficiency, and feasibility of heat balance, so as to develop a small, high-output electric motor in a short time. This paper outlines this analysis technology.

1. Challenges in designing electric motor with high torque density

Heat dissipation/cooling is an issue in downsizing an electric motor with high output. In electric motors, heat is generated by copper loss, iron loss, and mechanical loss. Downsizing an electric motor decreases the heat transfer area for heat dissipation, which raises the internal temperature, making its coil more susceptible to burn out. This temperature rise increases the resistance value of the coil, which causes the copper loss to increase, leading to a further rise in temperature. In addition, the rising internal temperature causes the thermal demagnetization of the magnet, leading to a decrease in the output.¹⁾ Moreover, the electromagnetic-steel sheet used for iron cores tends to experience increased iron loss when stress is applied.²⁾ Therefore, it is possible that the iron loss is increased due not only to the residual stress at the time of forming such as punching,³⁾ but also to the change in thermal stress caused by the rise in internal temperature.

Furthermore, the increase in iron loss also lowers the output torque of the electric motor.^{1), 4)} Current control by an inverter to maintain the target output torque results in an increased input current, further increasing the above-mentioned copper loss, iron loss, and temperature rise, making it difficult to achieve the target output performance.

Thus, in the design of an electric motor with high torque, it is necessary to consider electromagnetic design and heat transfer design as a coupled problem to be optimized. One means for performing this is a magnetic field analysis and heat transfer analysis using three-dimensional FEM. Coupling these two analyses to derive the optimum solution, however, results in a high calculation load and does not necessarily facilitate the study of the design change.

To solve these problems, Kobe Steel has used an electromagnetic field analysis method based on

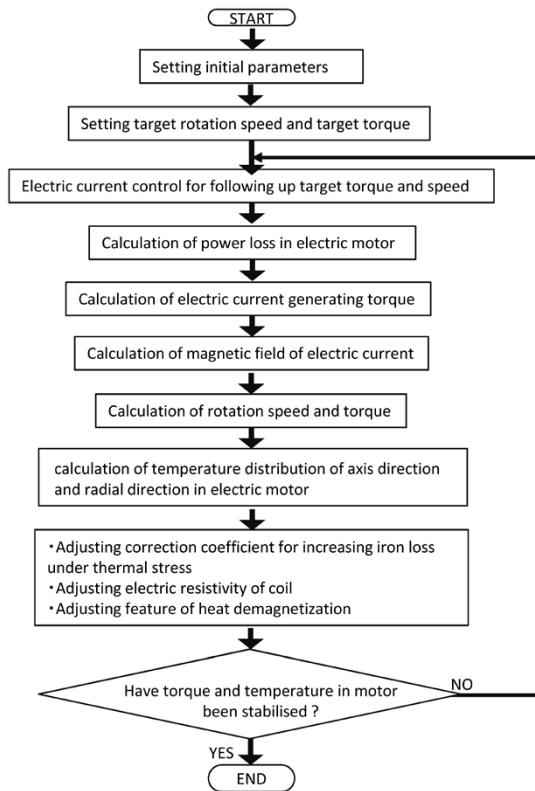


Fig. 1 Process of coupled simulation for electromagnetic circuit and heat transfer

the voltage equations for conventional motors and magnetic circuit calculations in accordance with the permeance method,⁴⁾ incorporating therein a process of calculating the amount of heat generated considering the temperature dependence of copper loss and stress dependence of iron loss. A simple analysis technique (Fig. 1) was also established to enable the electromagnetic circuit designing of an electric motor while visualizing the two-dimensional heat transfer state and temperature distribution in the axial direction and radial direction inside the electric motor. A small, high-output electric motor satisfying the requirements for the new hybrid excavator has been realized by utilizing this simple analysis technique. The following explains the calculation method for each loss and analytical model of heat transfer in this simplified analysis technique.

2. Calculating amount of heat generated inside electric motor

2.1 Calculating iron loss of stator iron-core and rotor iron-core

Iron loss is the main heat generation factor of the stator iron-core, rotor iron-core, and magnet of an electric motor. The calculation method adopted was the Steinmetz empirical equation (Equation (1)),

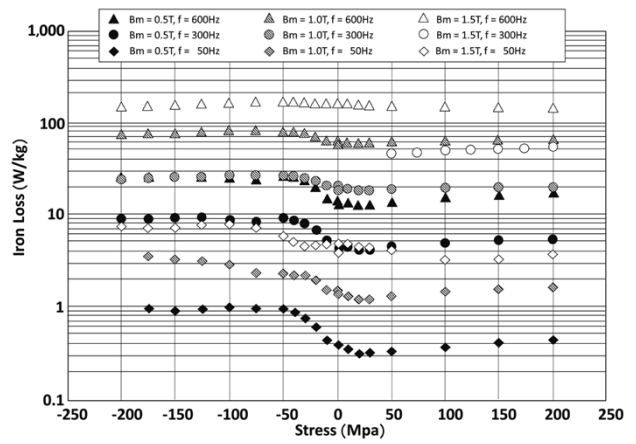


Fig. 2 Relationship between stress and iron loss

which takes into account the influence of frequency and magnetic flux density on both the hysteresis loss, W_h , and eddy current loss, W_e ;

$$W_F = W_h + W_e = K_h f B_m^{1.6} + K_e \frac{(t f B_m)^2}{\rho} \dots \dots \dots (1)$$

wherein W_F is iron loss; W_h , hysteresis loss; W_e , eddy current loss; K_h , hysteresis loss coefficient; K_e , eddy current loss coefficient; t , iron plate thickness; ρ , the resistivity of the magnetic body; and B_m , the maximum magnetic flux density of the magnetic flux currently occurring.

The proportion factors K_h and K_e/ρ of hysteresis loss and eddy current loss, respectively, are determined on the basis of the data for high-frequency iron loss curves, published by the manufacturers of electromagnetic steel sheets, to organize the relation between frequency and magnetic flux density. This equation is regarded as the basic equation.

On the other hand, the hysteresis loss and eddy current loss of an iron core increase with stress⁵⁾, which must be taken into account. For this reason, as shown in Equation (2), the correction factors K_{fh} and K_{fe} are incorporated into Equation (1) to increase each loss in accordance with the stress change, and, at the same time, the characteristics of iron loss change are evaluated by a stress test (Fig. 2) so as to change K_{fh} and K_{fe} with the increase/decrease ratio of the loss in accordance with the stress change to calculate the iron loss.

$$W_F = K_h K_{fh} f B_m^{1.6} + K_e K_{fe} \frac{(t f B_m)^2}{\rho} \dots \dots \dots (2)$$

wherein K_{fh} is the correction factor for hysteresis loss, and K_{fe} is the correction factor for eddy current loss.

The iron loss is calculated by applying Equation (2) of iron loss calculation to the three parts, namely, stator yoke, stator teeth, and rotor core. In the case of the iron core, the stress changes due to thermal expansion; to take this into account, a thermal stress analysis was conducted in advance in order to

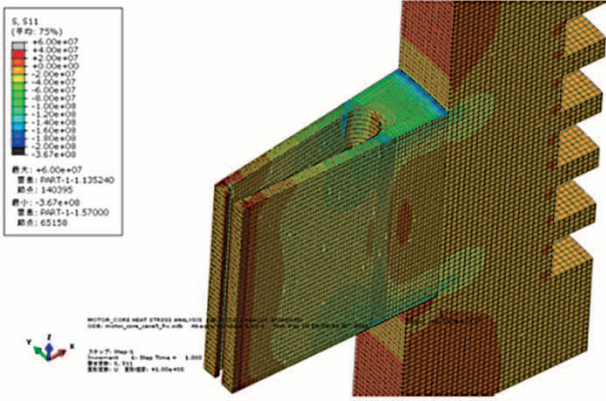


Fig. 3 Thermal stress distribution

understand the stress change and its distribution characteristics against temperature change (Fig. 3). Next, a calculation was performed to correct the stress value in accordance with the temperature change for the three divided parts, the yoke, teeth, and rotor.

2.2 Calculating copper loss of coil

The electric resistance of copper adopted to the coils of electric motors increases at a ratio of $0.39\%/^{\circ}\text{C}$; hence the copper loss is calculated by Equation (3).

$$W_c = R_{20} \{1 + 0.0039(T - 20)\} I^2 \dots\dots\dots (3)$$

wherein W_c is the copper loss (W), R_{20} is the resistance (Ω) at 20°C , T is the coil temperature ($^{\circ}\text{C}$), and I is the electric current (A).

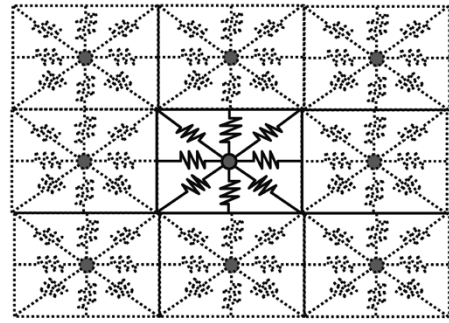
2.3 Mechanical loss including bearing loss and windage loss

The bearing loss and amount of heat generation are calculated on the basis of formulae⁶⁾ published by a bearing manufacturer. The windage loss is calculated by the product of the circumferential velocity and the viscosity coefficient determined in accordance with the rotor surface area.

3. Heat-transfer calculation model for electric motor

3.1 Basic model for heat-transfer calculation

In this paper, Microsoft EXCEL is used as a platform for establishing the analysis environment to analyze various losses and distributions inside an electric motor computed by electromagnetic simulation, as well as the heat transfer state and the temperature distribution inside the electric motor with its losses as the sources of heat generation.

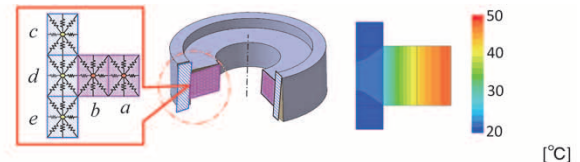


$$Q[W] = \frac{T_H - T_L}{R}$$

$$R[^{\circ}\text{C}/W] = \frac{L}{\lambda S}$$

T_H, T_L : Nodes
 R : Thermal resistance
 L : Heat transfer distance
 S : Cross-sectional area
 λ : Thermal conductivity
 Q : Amount of heat

Fig. 4 Element model for heat transfer simulation



Temperature	T_a	T_b	T_c	T_d	T_e
Proposal simulation	42.4	31.3	20.4	21.9	20.4
FEM analysis	45.4	34.7	20.6	21.7	20.5
Difference	3.1	3.4	0.1	-0.2	0.1

※Each temperatures in this table are averages of each elements.

Fig. 5 Comparison of temperatures between proposed model and FEM analysis

Excel is suitable for preparing a process of describing an arithmetic expression in each cell to calculate the influence of adjacent cells. In the cases where shapes are changed frequently as in the case of electric motor designing, the software is convenient for easily coping with the changes in shapes and heat transfer circuits by copying and pasting cells. Therefore, a basic model of heat-transfer calculation was prepared, regarding each cell of Excel as a basic element of the heat transfer circuit (Fig. 4). In this figure, each rectangle is a basic element dividing the heat transfer circuit. Using the Excel cells for this rectangle enables the expression of the heat transfer characteristics between adjacent basic elements (cells). For the preliminary verification, thermal conduction was calculated for an assumed electric motor as shown in Fig. 5. For the calculation, a heat generation amount of 200 W was set for each coil-equivalent part (parts a, b), and the temperature of the circumferential surface of the hollow cylinder (parts c, d, and e; material, aluminum) was fixed at 20°C . Comparing the results of this calculation with those of the FEM analysis has confirmed that the difference is approximately 3°C .

3.2 Heat transfer model of coil part

As shown in Fig. 6, the coil part in the slot of an electric motor stator is composed of multiple materials such as copper wire, insulation coating, filler for the voids created by copper wire, insulation paper, air, and iron core. This analysis is devised to calculate this composite member structure as one member using the heat transfer model of Fig. 4 as the base. The equivalent thermal resistance in the axial direction of the electric-motor with this composite structure can be regarded as the synthetic resistance of each parallel circuit of the thermal resistance of the corresponding member; and the equivalent thermal conductivity, λ_H , in the axial direction of the electric motor can be calculated by Equations (4). On the other hand, the equivalent thermal resistance in the radial direction of the electric motor can be regarded as the synthetic resistance of the series circuit of the thermal resistance of each member, and the equivalent thermal conductivity, λ_L , of the electric motor in the radial direction can be calculated by Equations (5).

$$\begin{cases} \frac{1}{R_H} = \frac{1}{R_{H,1}} + \frac{1}{R_{H,2}} + \frac{1}{R_{H,3}} + \frac{1}{R_{H,4}} & \dots\dots\dots (4) \\ R_H = \frac{H}{\lambda_H A_0}, R_{H,i} = \frac{H}{\lambda_i A_i} (i=1, 2, 3, 4) \end{cases}$$

$$\begin{cases} R_L = R_{L,1} + R_{L,2} + R_{L,3} + R_{L,4} \\ R_L \doteq \frac{A_0}{\lambda_L H W^2}, R_{L,i} \doteq \frac{A_i}{\lambda_i H W^2} (i=1, 2, 3, 4) & \dots\dots\dots (5) \end{cases}$$

wherein

- R_H : the equivalent thermal resistance in the axial direction of the coil composite structure,
- $R_{H,i}$: the thermal resistance in the axial direction of each material in the coil composite structure,
- R_L : the equivalent thermal resistance in the radial direction of the coil composite structure,
- $R_{L,i}$: the thermal resistance in the radial direction

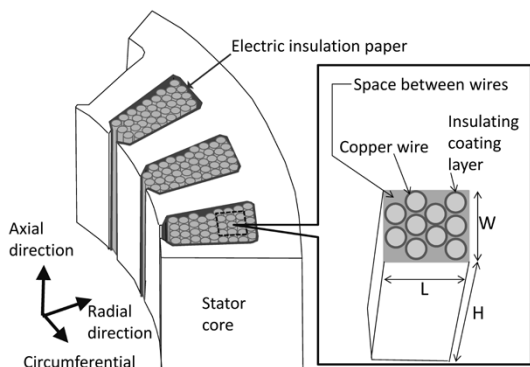


Fig. 6 Coil structure

of each material in the coil composite structure,

- λ_H : the equivalent thermal conductivity in the axial direction of the coil composite structure,
- λ_L : the equivalent thermal conductivity in the radial direction of the coil composite structure,
- λ_i : the conductivity of each material in the coil composite structure,
- A_0 : the cross-sectional area of the coil composite structure,
- A_i : the cross-sectional area of each material in the coil composite structure,
- $i=1$, for copper wire; $=2$, for insulation coating; $=3$, for copper wire; $=4$, for voids.

Regarding the coil part of the electric motor as one member with different equivalent thermal conductivities λ_H and λ_L in the axial and the radial directions has simplified the heat-transfer calculation. It should be noted that, when each material itself has different thermal conductivities in the axial and the radial directions, the equivalent thermal conductivity must be calculated using the respective thermal conductivity.

3.3 Heat transfer model of bearing

In a bearing in its stopped state, heat is transferred from the outer surface on the high temperature side of each rolling body to the inside, and further to the surface on the low temperature side, causing a heat transfer between the inner ring and the outer ring. When a bearing is rolling, each part of the outer surface of the rolling body contacts the inner ring and the outer ring alternately, thus causing thermal conduction. Therefore, the heat transfer model in Fig. 4 was used as the base to prepare a model for thermal conduction, in which the heat accumulated on the outer surface of the rolling body is thermally conducted between the inner ring and the outer ring without being conducted through inside the rolling body (Fig. 7). The rolling body was simulated with 4 point elements on its surface, and 1 point element at its center, in which the four elements on the surface have thermal resistance on the sides of both the inner ring and outer ring; and the thermal resistance of the element in contact with the inner ring or the outer ring, depending on the rotation of the rolling body, is given a small thermal resistance value, while the thermal resistance of the element not in contact is switched to a large value, thereby enabling the calculation of the thermal conduction at the surface of the rolling body.

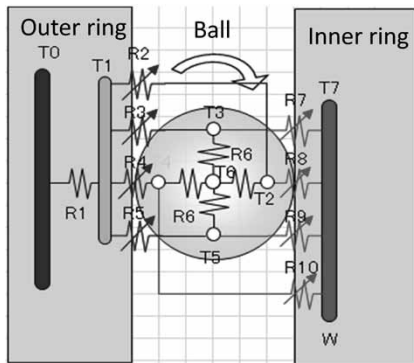
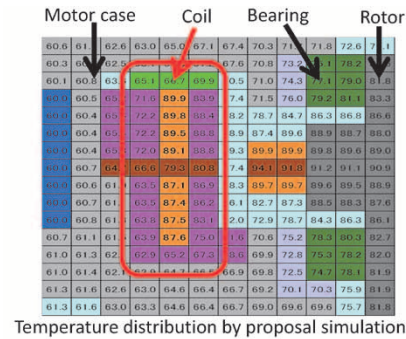


Fig. 7 Heat transfer model of ball bearing

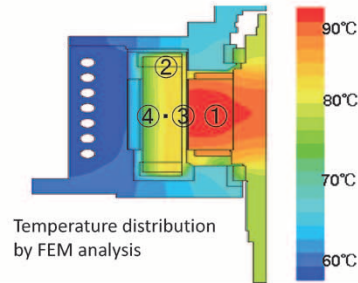
4. Coupled simulation of electricity magnetism and heat transfer

In an electric motor, a part of the input power is consumed as a copper loss and/or iron loss. In particular, the iron loss consumes a part of the electric current to be converted to output torque, and an increase in iron loss causes a decrease in output torque. Therefore, it is necessary to increase the input electric current to output the target torque. In order to determine the substantially necessary input electric current considering the above, following the chart in Fig. 1, the magnetic flux and electric current in the electromagnetic circuit inside the electric motor are calculated, while the iron loss, copper loss, and bearing loss are calculated as above, to arrive at the output torque considering the influence of each loss. Then, the input electric current is increased for the decrease in the output torque with respect to the target torque by operating the input electric current control. These iterative calculations are repeated until the output torque is stabilized at the target value and the temperature of each part of the electric motor is also stabilized. The results of this calculation allow the prediction of how the heat generated by iron loss, copper loss, and mechanical loss, occurring in each part of the electric motor, is transferred to the cooling section of the electric motor housing via the heat transfer route of the structural members of the electric motor and the air layer in its inner space. As a result, it is possible to optimally design the electromagnetic circuit and heat transfer circuit that meets the target output performance and target temperature of an electric motor. This coupled simulation environment has been used to design a small electric motor with high output for a hybrid excavator. Furthermore, after simulation confirmed that the target performance is achievable, an electric motor was prototyped to verify the output performance, efficiency, and feasibility of heat balance.

The coupled simulation constructed this time



Temperature distribution by proposal simulation



Temperature distribution by FEM analysis

	Proposal simulation	FEM
①Rotor [°C]	93.0	92.0
②Coil end[°C]	89.9	84.7
③Coil in slot[°C]	85.7	80.7
④Teeth[°C]	80.8	83.9

Fig. 8 Comparison of heat transfer between proposed simulation and FEM analysis

was used to calculate the internal temperature distribution at the rated output of the slewing electric motor that was designed. Fig. 8 shows the results of the computation. For comparison, FEM analysis was also carried out to confirm validity.

The efficiency distribution calculation results of all output region will be described in the next section.

5. Performance evaluation of electric motor design

Due to space limitations, this paper reports only the evaluation results for the slewing electric motor prototyped. An electric motor designed to have the performance confirmed by the simulation described above was prototyped (Fig. 9). Heat balance testing for verification by comparison with the analysis result of Fig. 8 and the efficiency distribution measurement in the whole output range were carried out on a motor bench apparatus.

A heat balance test was carried out at a rated output condition, and the results show that the temperature distribution inside the electric motor tends to be approximated to the analysis, although the in-slot coil temperature became 10 to 13°C higher than the analysis results (Fig.10). Moreover, there is a good agreement between the analysis results of efficiency distribution for the entire output range



Fig. 9 Prototyped motor of slewing motion

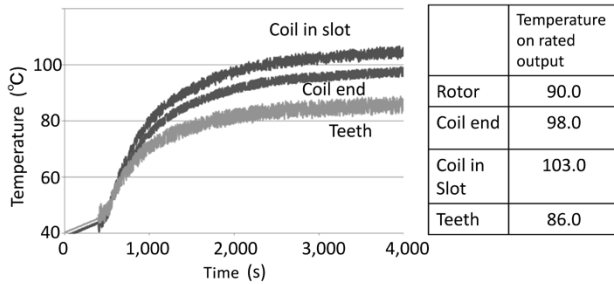


Fig.10 Experimental results of heat balance of prototyped electric motor

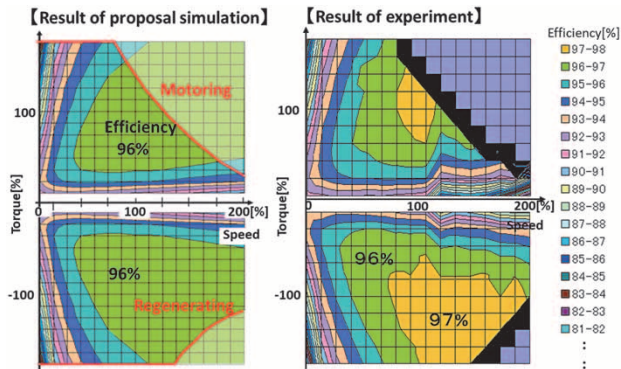


Fig.11 Comparison of efficiency distribution of prototyped motor between simulation and experimental results

and experimental results (Fig.11), confirming that the highest efficiency can be predicted.

Conclusions

This paper has focused on the issues of heat generation, heat extraction and heat transfer, which poses problems in the designing of a compact electric motor with high output and torque, and introduced a coupled analysis technology for electricity magnetism and heat transfer, the technology established to find the structural design for removing heat generated inside a motor to the outside with a minimum heat transfer and radiation area. This technology has led to the successful development of a small, high-output slewing electric motor for hybrid excavator and a flat high-torque generator motor.

There still will be a need for further performance upgrading of electric motors and lead-time reduction of the development. We will strive to advance the development of analytical prediction technologies.

References

- 1) D. Ebihara . *Mōta gijutsu jitsuyō handobukku 1st edition*. 2001, p.419, p.692.
- 2) J. Magn. *Sec. Jpn.* 2006, Vol.30, pp.196-200.
- 3) J. Toda et al. *JFE Technical Report*. 2015, No.36, pp.24-31.
- 4) Y. Takeda et al. *Umekomi jishaku dōki mōta no sekkei to seigyō 1st edition*. Ohmsha, 2001, p.17, pp.74-84.
- 5) K. Narita. *JMAG Newsletter*. January 2014, pp.37-41.
- 6) *Roller bearing general catalog (Cat. No.2202/J)*. NTN Corporation, p.A-71.